Journal of Non-Crystalline Solids 408 (2015) 76–86

Contents lists available at ScienceDirect

Journal of Non-Crystalline Solids

journal homepage: www.elsevier.com/ locate/ jnoncrysol

Viscosity profiles of phosphate glasses through combined quasi-static and bob-in-cup methods

A.J. Parsons [a,*], N. Sharmin [a], Sharifah I.S. Shaharuddin [a], M. Marshall [b]

[a] Division of MMS, Faculty of Engineering, University of Nottingham, NG7 2RD, UK
[b] Glass Technology Services, 9 Churchill Way, Sheffield, South Yorkshire, S35 2PY, UK

ARTICLE INFO

Article history:
Received 15 July 2014
Received in revised form 13 October 2014
Accepted 15 October 2014
Available online 25 October 2014

Classification codes:
Glasses rheology (83.80.Ab);
Glasses thermal properties (65.60. + a)

JNCS classification codes:
190: Glasses;
470.300: Glass transition;
480.700: Viscosity

Keywords:
Phosphate glass;
Viscosity;
Vogel–Fulcher–Tammann;
Fragility

ABSTRACT

This study used a combined viscosity approach to determine theoretical fibre drawing points for glasses in the series: xP_2O_5, 24MgO, 16CaO, (60-x)Na_2O (x = 40,45,50,55) and yP_2O_5, 24MgO, 16CaO, (55-y)Na_2O, $5Fe_2O_3$ (y = 40,45,50,55). The points cannot be measured directly since the glasses are only kinetically stable at these points and would crystallise if allowed to equilibrate. Quasi-static and bob-in-cup viscosity data from above and below the range of interest were fitted to the Vogel–Fulcher–Tammann equation and provided good agreement. The theoretical drawing points were taken as the temperature at which the glass has a viscosity of 2 Log Pa·s, based on the known drawing point viscosity of silica glasses. The theoretical drawing points for the glasses ranged from 657 to 839 °C. The viscosity information was also used to assess the fragility of the glasses in comparison with a borosilicate standard by using Doremus and Angell parameters. All of the glasses were of low viscosity and high fragility in comparison to the borosilicate. The fragility improved above 50% content of phosphate in the glass and the addition of iron had little effect on the fragility. Additionally, the limitations of the borosilicate 717a standard glass and the measurement of T_g are discussed.

1. Introduction

Phosphate glasses and their fibres are being developed for use in medical applications [1–3]. This is because they possess relatively high strength values (typically 500 MPa to 1.2 GPa [4]) but can also degrade away in an aqueous environment. Ordinarily this is a surface erosion process [5], allowing for the maintenance of properties during degradation [6].

The glasses can be utilised both directly and as reinforcements in composite materials. To make use of the strength properties of the glasses when reinforcing composites, it is necessary to have them in the form of fibres. The production of phosphate optical fibres via pre-form drawing processes is well known [7], but to create reinforcing fibres for composites these processes are not well suited. Typical optical fibres are in the range >30 μm and often in the hundreds of microns; a desirable diameter for reinforcing fibres is <25 μm and preferably ~9–12 μm [8]. Additionally, reinforcing fibres are created as multi-filament tows that contain hundreds and often thousands of individual filaments all drawn at the same time, making pre-form drawing impractical (although not impossible). To create small diameter, multi-filament threads it is necessary to use melt drawing.

Melt drawing is also well known, though overwhelmingly focused on silica-based glasses. Silica fibres (commonly E-glass) have been produced on a commercial scale since the 1960s [9]. However, a commercial process for small diameter phosphate glass fibre production has never been achieved. This is partially due to a lack of perceived applications for phosphate glass fibres until relatively recently and partly due to the properties of the glass.

Silica bases glasses draw very effectively in the commercial melt drawing process because they possess viscosities at the appropriate level for fibre production when the glass is above its liquidus [10]. This means that the molten glass can be held at the correct fibre drawing temperature without a risk of crystallisation and so a continuous process is possible.

Phosphate glasses tend to be fragile and prone to crystallisation, with viscosities much lower than silicates. Critically, the 'drawing point' viscosity for glass fibre production (typically assumed to be ~100 Pa·s or 2 Log Pa·s [10]) usually falls below the liquidus point and due to the fragility of the glasses the drawing point temperature window is also relatively narrow. Conventionally this would preclude melt-drawing but a number of groups around the world, including

* Corresponding author.
E-mail address: andrew.parsons@nottingham.ac.uk (A.J. Parsons).

http://dx.doi.org/10.1016/j.jnoncrysol.2014.10.014

ours, have been producing phosphate glass fibres successfully in the laboratory for many years. This is because glass that is flowing is more resistant to crystallisation, lending a kinetic stability to the process. As such a continuous production process is feasible but to design a long term, reliable process, good information about the viscosity of the glass is necessary. If correct conditions are not achieved and crystals nucleate then gradual growth of these crystals will occur, resulting in reduced quality fibre and eventual blockage of the drawing equipment.

Because the glasses are only usually kinetically stable at their drawing point temperatures it is impossible to take equilibrium viscosity measurements of the drawing point directly. In order to obtain close approximations of these values, this study combines parallel plate quasi-static viscosity measurements using Gent's equation [11] with high temperature bob-in-cup measurements that fall either side of the crystallisation region. Quasi-static measurements provide values in the range of 5.5–8 Log Pa·s, while bob-in-cup measurements provide values in the <2 Log Pa·s region. The data is then applied to the well-known and generally accepted Vogel–Fulcher–Tammann (VFT) equation (developed in the 1920s) in order to predict a complete viscosity profile and a drawing point temperature. Additionally, the viscosity data is combined with conventional thermal analysis methods to obtain Angell [12,13] and Doremus [14] fragility indices. The data also provides some insights to the effect of additives on the structure of phosphate glasses. The study includes eight glass formulations from the following two systems: xP_2O_5, 24MgO, 16CaO, (60-x)Na_2O (x = 40,45,50,55) and yP_2O_5, 24MgO, 16CaO, (55-y)Na_2O, $5Fe_2O_3$ (y = 40,45,50,55). The glasses were selected based on previously determined formulations with good cytocompatibility [15].

2. Methods

2.1. Glass production

Glasses were produced by melt fusing phosphate salts and phosphorus pentoxide in 5%Au/Pt crucibles. NaH_2PO_4, $CaHPO_4$, $MgHPO_4 \cdot 3H_2O$ and $FePO_4 \cdot 2H_2O$ were obtained from Sigma Aldrich UK, P_2O_5 was obtained from Fisher Chemicals. All Reagents were used as received. Each batch was heated for 30 min at 350 °C in a Lenton Furnaces AWF 12/26 to drive off adducted water before being transferred to a Lenton Furnaces UAF 16/10 at 1100 °C for 90 min. The glasses were either cast directly onto a steel plate or poured into 4 mm diameter graphite moulds. Glass compositions and precursor recipes can be found in Table 1.

2.2. Glass sample preparation

The glass cast directly was broken up into cullet and used for density and liquidus measurements, and bob-in-cup viscosity. The glass cast into the graphite moulds was annealed at the glass $T_g + 10$ °C as recommended by Ropp [16], before careful sectioning into parallel faced, ~3 mm long rods for quasi-static viscosity by using a South Bay Technologies Inc. Model 650 low speed diamond saw. Pieces of the glasses were also ground to powder for differential scanning calorimetry (DSC), using a Retch Planetary Ball Mill PM 100 with zirconia grinding surfaces. The average particle size was <45 μm (measured using calibrated testing sieves).

Table 1
Glass recipes.

Glass code (mol% oxide)	Precursor mixture (mass% ±0.01 g)				
	NaH_2PO_4	$FePO_4 \cdot 2H_2O$	$CaHPO_4$	$MgHPO_4 \cdot 3H_2O$	P_2O_5
P40Mg24Ca16Na20	43.00	0.00	19.51	37.49	0.00
P45Mg24Ca16Na15	31.63	0.00	19.13	36.77	12.48
P50Mg24Ca16Na10	20.69	0.00	18.77	36.07	24.48
P55Mg24Ca16Na5	10.15	0.00	18.42	35.40	36.03
P40Mg24Ca16Na15Fe5	30.43	15.80	18.40	35.37	0.00
P45Mg24Ca16Na10Fe5	19.92	15.51	18.07	34.73	11.78
P50Mg24Ca16Na5Fe5	9.78	15.23	17.74	34.10	23.14
P55Mg24Ca16Fe5	0.00	14.96	17.43	33.50	34.11

2.3. X-ray fluorescence spectroscopy (XRF)

XRF compositional analysis was carried out on a Bruker S4 Pioneer XRF set. Samples were prepared by re-melting the glass diluted with lithium tetraborate at 1220 °C and casting into platinum dishes. The resulting 40 mm diameter discs are then submitted for analysis, taking care to avoid any contamination from handling. Analysis is performed with the instrument operating in the "standard-less mode" which was developed internally for these types of non soda–lime–silica (SLS) glasses. Results which provide a total sample value outside of the 99.5–100.5% range (a total value of 100% is expected) are rejected and sampling and fusion is repeated.

2.4. Differential scanning calorimetry (DSC)

Thermal analysis of the glasses was performed using a Texas Instruments SDTQ600. Measurements of glass transition temperature were taken in triplicate at 10 °C/min using platinum pans containing ~30 mg of powdered glass.

2.5. Liquidus

Liquidus measurements were undertaken according to ASTM C829-81, using a purpose built furnace. Coarse glass cullet (3–5 mm) is placed into a 155 mm × 10 mm × 10 mm 90%Pt/10%Rh tray and melted at 1450 °C for 15 min in order to allow the glass to flow and fill the tray. The tray is then held in the liquidus furnace for 24 h to stabilise before being removed and cooled in air. The extent of crystallisation is determined by using an optical microscope and observing the centre of the resulting glass bar (some nucleation could occur at the walls). The thermal gradient in the furnace is determined by 15 thermocouples with a spacing of 10 mm and confirmed by using a movable thermocouple. The temperature gradient across the length of the sample is typically ~80 °C. An approximate temperature can be obtained from the DSC data in order to reduce experimental time.

2.6. Density

Glass density was measured using bubble free cullet in a Micromeritics AccuPyc 1330 gas pycnometer, using helium gas. The pycnometer was calibrated and checked by using steel calibration standards, with 10 measurements made. For the glass, 5 measurements were made for each of three different glass batches of each composition.

2.7. Quasi-static viscosity

The quasi-static viscosity data was obtained via a process described elsewhere [17–19]. Briefly, a small rod of the glass (4 mm diameter × 3 mm length) is subjected to a constant axial force while heated and the rate of change of height of the rod provides a viscosity vs temperature profile. The measurements were taken in triplicate for each composition.

2.8. Bob-in-cup viscosity

Bob-in-cup viscosity measurements were taken essentially in accordance with ISO 7884–2:1987 by using a Theta industries Rheotronic II 1600 °C Rotating Viscometer. The system uses a 10 mm diameter, 14 mm high platinum double cone bob in a 40 mm high, 30 mm internal diameter platinum crucible with a 1 mm wall thickness. The glass density was used to determine the amount of cullet required to achieve a glass height of ~24 mm in the crucible (with the bob inserted). The

system measures the shear stress using a Brookfield DV-III Ultra Rheometer and is calibrated by using a multiplication or 'spindle' factor based on a standard material.

Calibration was undertaken by use of the borosilicate glass standard reference material 717a. The glass was heated to 1256 °C and the bob lowered into the crucible to a height of 3 mm above the base. Sufficient spindle RPM was used to achieve >70% torque (10 rpm). Readings of the viscosity were taken every minute and a minimum determined (see discussion for more explanation). An appropriate spindle factor was then chosen to adjust the minimum viscosity reading to 100,000 cP, or Log Pa·s = 2, as per the values provided for the 717a standard.

To measure a sample, the system is heated to 1100 °C. After 30 min the platinum bob is lowered into the now molten glass so that the base of the bob is 3 mm above the base of the crucible. The system is then left for a further 15 min to come to thermal equilibrium. Viscosity measurements are taken at different RPM values, to probe the viscosity behaviour of the glass. The temperature is lowered in stages, with suitable equilibrium time allowance, until the glass either crystallises or the torque limits of the system are exceeded. Three different batches of each glass type were used. To check that there was no drift in the spring value over the course of the experiments, a fresh batch of the first glass tested was run again at the end. The equipment uses known geometric values and the calibration constant to provide values in cP, which were converted to Log Pa·s.

3. Results

3.1. XRF analysis

XRF analysis of the final glass compositions are provided in Table 2, alongside the expected feed compositions. Values are in mol%. In all cases except for the Na_2O in P40Mg24Ca16Na15Fe5 the results were within 1% of expectation and in the majority of cases within 0.5%, giving good confidence in the composition of the glasses.

3.2. Thermal analysis and density

Glass transition temperature, liquidus and density values for the different glasses are provided in Table 3. Density values drop with increasing phosphate content, and the density increases with iron addition. T_g values show a general trend of increase with phosphate content but with unusual non-linearity. Liquidus values are distinctly non-linear and do not seem to follow a pattern.

3.3. Quasi-static viscosity

Quasi-static viscosity data is provided in Fig. 1. All the glasses showed reasonably linear behaviour in the region of 5.5 to 8 Log Pa·s ($R^2 > 0.99$). Viscosity increased with increasing phosphate content.

Table 3
Thermal data and density.

Glass code (mol% oxide)	T_g (°C)	Liquidus (°C)	Density (kg/m3)
P40Mg24Ca16Na20	443 ± 1	900 ± 5	2689 ± 1
P45Mg24Ca16Na15	450 ± 1	822 ± 5	2641 ± 1
P50Mg24Ca16Na10	465 ± 3	863 ± 5	2588 ± 1
P55Mg24Ca16Na5	460 ± 2	974 ± 5	2536 ± 2
P40Mg24Ca16Na15Fe5	496 ± 2	925 ± 5	2821 ± 1
P45Mg24Ca16Na10Fe5	490 ± 2	957 ± 5	2765 ± 1
P50Mg24Ca16Na5Fe5	501 ± 2	877 ± 5	2698 ± 2
P55Mg24Ca16Fe5	521 ± 2	1000 ± 5	2621 ± 1

However, the addition of iron increased the viscosity of the glass greatly, with even the P40Mg24Ca16Na15Fe5 glass demonstrating a higher viscosity than the P55Mg24Ca16Na5 glass. This indicates that iron has a greater effect on the viscosity of these glasses than phosphate content in this viscosity range. Additionally, the magnitude of the effect of increasing phosphorus is different between the glasses containing Fe and those not — there is almost no difference in viscosity between P50Mg24Ca16Na10 and P55Mg24Ca16Na5 in this region, whereas the jump between P50Mg24Ca16Na5Fe5 and P55Mg24Ca16Fe5 is the most significant in that series, though the P55Mg24Ca16Fe5 does contain no sodium. Furthermore, a gradual reduction in gradient is observed for the high phosphate content glasses, suggesting an improvement in glass fragility.

3.4. Bob-in-cup viscosity

3.4.1. Newtonian behaviour of phosphate glasses

The viscosity of the glasses was measured for a range of RPM values at each temperature, which in turn affected the shear rate and shear stress. For all of the glasses the viscosity was constant within error for RPM values of 10 or above and the glasses are considered to be Newtonian. For the P50 glasses, crystallisation did not appear to occur until relatively low temperatures were achieved and RPM values of below 10 were required to remain below 100% torque. In these instances there was some divergence in the value of viscosity for different RPM values. This was surmised to be due to slow crystallisation and the results were discounted.

3.4.2. Viscosity data

Bob in cup data is provided in Fig. 2. The glasses showed good linearity over the range of measurement (P40s and P55s $R^2 > 0.99$, P45s $R^2 > 0.98$, P50s $R^2 > 0.97$). Once again, viscosity is seen to increase with increasing phosphate content. However, in this region of viscosity the phosphorus seems to have a much greater effect than the iron. In Fig. 1 the iron containing range of glasses all had higher viscosities than the non-iron containing range. In Fig. 2 the iron and non-iron pairs are quite close together, with a clear split between each level of phosphate content (e.g. P40Mg24Ca16Na20 and P40Mg24Ca16Na15Fe5

Table 2
Glass compositional analysis.

Oxide	Expected	XRF (±0.5)	Expected	XRF (±0.5)	Expected	XRF (±0.5)	Expected	XRF (±0.5)
	P40Mg24Ca16Na20		P45Mg24Ca16Na15		P50Mg24Ca16Na10		P55Mg24Ca16Na5	
P_2O_5	40	39.8	45	45.1	50	49.4	55	54.0
MgO	24	23.9	24	23.8	24	23.6	24	24.0
CaO	16	16.2	16	16.3	16	16.2	16	16.4
Fe_2O_3	0	0.0	0	0.0	0	0.0	0	0.0
Na_2O	20	20.0	15	14.7	10	10.7	5	5.6
	P40Mg24Ca16Na15Fe5		P45Mg24Ca16Na10Fe5		P50Mg24Ca16Na5Fe5		P55Mg24Ca16Fe5	
P_2O_5	40	39.3	45	44.7	50	49.6	55	54.3
MgO	24	23.5	24	23.7	24	24.1	24	24.4
CaO	16	16.3	16	16.4	16	16.5	16	16.4
Fe_2O_3	5	4.6	5	4.8	5	4.8	5	4.9
Na_2O	15	16.3	10	10.4	5	5.0	0	0.0

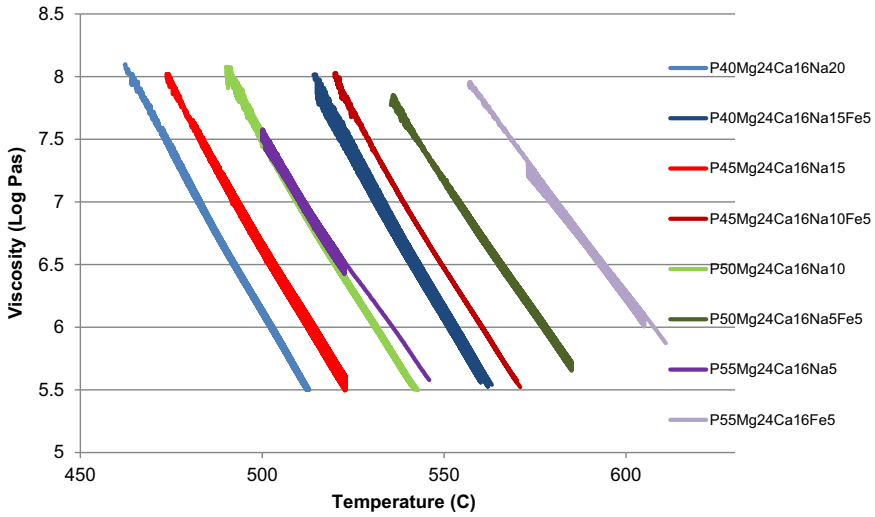

Fig. 1. Viscosity of the glasses in the range 5.5 to 8 Log Pa·s obtained through the quasi-static parallel plate method. The data shown includes three measurements for each glass type, demonstrating the degree of repeatability. Error bars are omitted for clarity, though the assumed error is ±0.2 Log Pa·s.

lie close together and are below both the P50 glasses). Additionally, the presence of iron seems to have a greater effect on the viscosity at higher phosphate levels.

4. Discussion

4.1. Thermal analysis and density

The T_g values shown in Table 3 generally increase both with increasing phosphate content (due to increasing phosphate chain length) and with increasing iron content (due to cross linking [20]), as would be expected. Above P50 there is a degree of branching, which can perturb the structure and reduce the T_g again, which could explain the peak in T_g at P50 for the non-iron containing glasses. With the iron containing glasses, the effect of iron largely overrides the effect of phosphate in the shorter chain systems and the high value of P55Mg24Ca16Fe5 is likely to be due to the complete absence of sodium as a modifier.

Density also goes up with iron content (as expected [21]) but down with phosphate content. Reduced density occurs in longer chain length glasses due to increasing difficulty in chain packing. The liquidus values do not show an obvious pattern and the reasons for this are not clear. Further analysis of the liquidus surface of these glass compositions would be of benefit in future studies as there may be a eutectic effect.

4.2. Viscosity analysis

4.2.1. Limitations in the measurement of viscosity of phosphate glasses at high temperature and consideration of error

Due to the prevalence of silica based glasses and the relative obscurity of phosphate glasses, the high temperature viscosity equipment and, critically, the related standard materials are intended primarily for the measurement of the former glass type. While the process is applicable directly to phosphate glasses, there are limitations to consider.

When calibrating a viscometer it is advisable to select a standard material that has a comparable viscosity profile, so as to ensure that measurements are made in a similar range of torque. For glass viscosity, there are a very limited number of standard glasses available with certified values for Log Pa·s = 2 and these are all silica based glasses

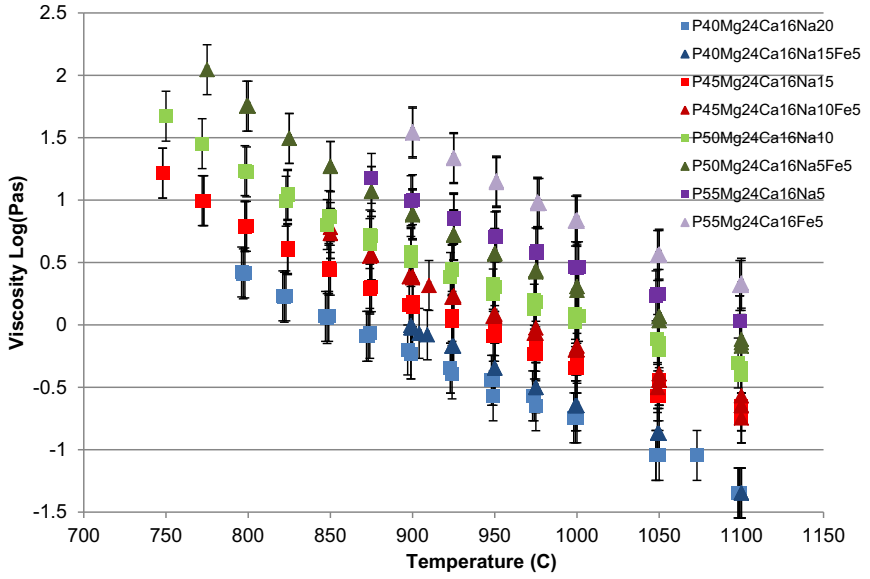

Fig. 2. Viscosity for the glasses in the range −1.5 to 2 Log Pa·s obtained through the bob in cup method. The data shown includes three measurements for each glass type demonstrating the degree of repeatability. Errors are taken to be ±0.2 Log Pa·s.

with viscosities typically an order of magnitude or more higher than phosphate glasses at equivalent temperatures. For the fragile phosphate glasses, where measurements are being made at Log Pa·s < 2 this means that torque values can be very low and in some cases less than the recommended minimum for the equipment of 10% torque. As such, error levels for individual readings are likely to be higher than might otherwise be expected. Having said that, triplicate measurements for three different batches of each glass provided very good repeatability and give confidence in the results. Additionally, the final batch run to check for drift in the machine gave a very good match to the first glass, demonstrating good stability in the equipment over several months. Overall error in repeatability of the data is of the order of 0.1 Log Pa·s. This error is in addition to the systematic error provided for the viscosity standard, which is listed as 2.00 ± 0.10 Log Pa·s at 1256 °C. Error in the furnace temperature is comparatively negligible. We will take the overall error to be ±0.2 Log Pa·s.

The standard reference material provided for the calibration of the equipment was the 717a borosilicate glass. The standard notes that the glass is susceptible to volatilisation at high temperatures but suggest that this is only of real concern above 1400 °C. However, trials in this study determined that the viscosity of this glass is quite variable, even at 1256 °C. This is problematic, since when measuring viscosity the recommendation is to allow a considerable length of time to achieve equilibrium. The standard does not provide guidelines as to how long the material should be held at temperature before taking a measurement and reference to the original papers on the standard glasses does not provide this parameter explicitly either. It can be inferred from the papers that the time before measurement is relatively short [22,23].

After a number of measurements, the authors would recommend that when using this calibration glass a rapid heating rate is used to achieve temperature, followed by a continuous monitoring of the viscosity in order to achieve a minimum, as shown in Fig. 3.

This minimum is then taken to be the viscosity at that temperature. Prior to the minimum the glass has not quite achieved the set temperature and so the viscosity is falling. After the minimum the loss of light components (B and possibly Na) becomes the dominant factor and so the viscosity increases. The result is repeatable but the faster the heating rate the better. A slower heating rate results in a convergence with the curve but at a higher minimum, indicating that material loss has already occurred before reaching temperature. A minimum is taken rather than an extrapolation for two reasons. Firstly, the minimum approach is closer to the method used in the papers on the standard glass, i.e. a measurement taken shortly after reaching temperature. Secondly, the temperature of the glass is not measured directly, so it is difficult to determine a '0 min' point. Overall one must consider that the viscosity will be slightly higher than the true value since it is not possible to heat the glass instantaneously and a safe limit for the equipment is considered to be 20 °C/min. Fortunately, the phosphate glasses do not appear to show this instability and it is possible to obtain stable equilibrium measurements, at least below 1100 °C.

Unfortunately 710a soda lime silica and 711 lead glass viscosity standards have been discontinued and so their suitability cannot be considered. It would be greatly beneficial to phosphate glass researchers for a phosphate glass viscosity standard to be established and it is important to highlight the limitations of the 717a calibration material to other users.

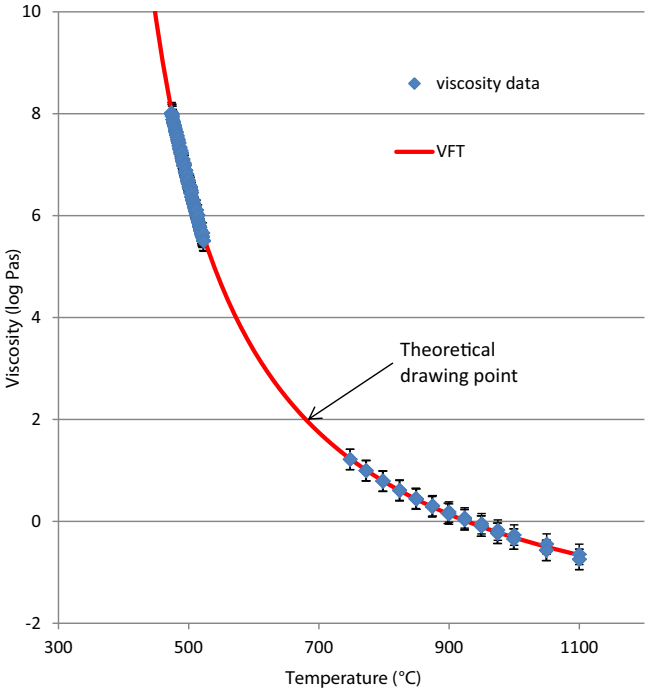

Fig. 4. Example of the fit of the viscosity data to the Vogel–Fulcher–Tammann equation, showing good agreement.

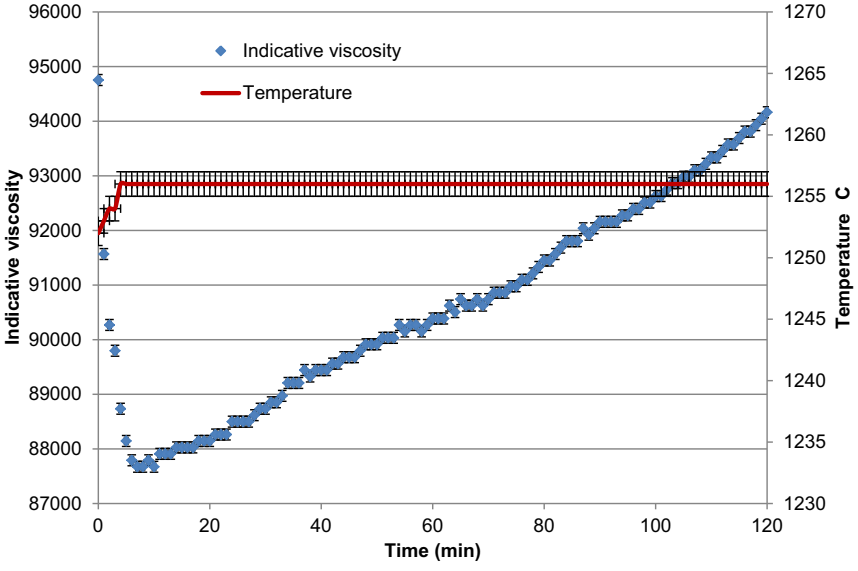

Fig. 3. Variation in the viscosity of the calibration glass with time when held at constant temperature.

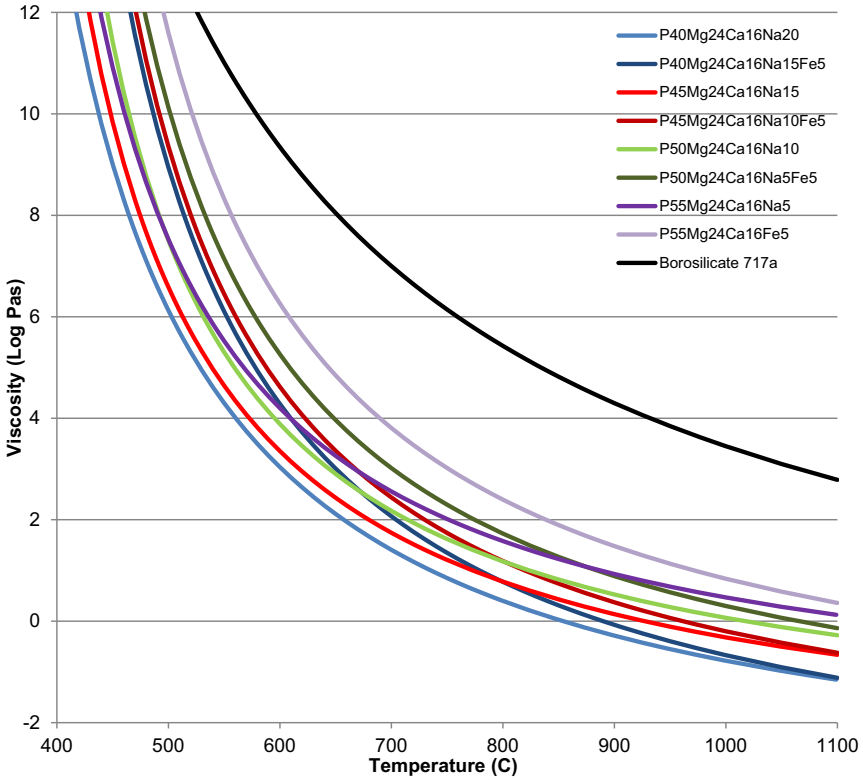

Fig. 5. Combined viscosity profiles fitted using the Vogel–Fulcher–Tammann equation, with the standard glass 717a for comparison. Errors are taken to be ±0.2 Log Pa·s.

Finally, the surface tension of glasses decreases with temperature, providing a practical limit above which the glass will creep up the spindle and cause damage to the supporting components. For the Pt alloy and the glasses used in the study a limit of 1100 °C was imposed. Moving to a Au/Pt low wetting alloy may provide a greater window of measurement.

4.2.2. Combination of viscosity data and application of models

In order to obtain a complete picture of the viscosity profile the quasi static data and bob-in-cup data were combined. There are a number of potential fits for viscosity and Ojovan provides a useful review [24]. This study will be limited to the Vogel–Fulcher–Tammann (VFT) equation (Eq. (1)), which is considered to have the best fit across the full spectrum of viscosity.

$$\mathrm{Log}\ (\eta) = A + \frac{B}{T - T_0} \quad (1)$$

The Excel Solver addin was used to fit the values of A, B and T_0 by a least squares regression method. An example of the data fit is provided in Fig. 4 and the combined graphs are provided in Fig. 5, with the values of A, B, and T_o, the theoretical drawing point (i.e. the value of temperature at a viscosity of Log Pa·s = 2) (T_D) and the difference between drawing point and liquidus (ΔT) provided in Table 4.

As was considered in Sections 3.3 and 3.4.2, it is apparent from Fig. 5 that the effect of iron on the viscosity of the glass varies. At lower temperature, i.e. higher viscosity, there is a significant increase in viscosity provided by the presence of iron (which is also reflected in the values of T_g in Table 3). At higher temperatures the traces converge, with the presence of iron providing little difference in the viscosity. For greater clarity, the P40 pair are extracted from Fig. 5 and shown in Fig. 6 as an example. This trend appears to be the case for all the glasses from P40 to P55. The reason for this bears further investigation and may be related to the mobility of the Fe^{3+} ion at higher temperature. However, structural analysis of the glasses is beyond the scope of the present study.

There is a small but distinct increase in viscosity of the glasses with increasing phosphate content between 40% and 50%, as might be expected with an increasing phosphate chain length. However the 55% phosphate glass appears to behave in a different fashion, with a more pronounced effect at high temperature but only a small effect or no effect at low temperature (c.f. Figs. 1 and 2). This seems to be the opposite effect to the presence of iron. Again, this bears further investigation but is likely related to the level of branching in the phosphate. It is interesting to note that this effect is not seen in the 55% phosphate containing

Table 4
VFT parameters and drawing points.

Glass code (mol% oxide)	A (±0.1)	B (±100)	To (±10)	T_D (°C)	Liquidus (°C)	ΔT (°C)
P40Mg24Ca16Na20	−3.9	2233	277	657 ± 3%	900 ± 5	−243 ± 8
P45Mg24Ca16Na15	−3.1	1912	302	680 ± 4%	822 ± 5	−142 ± 6
P50Mg24Ca16Na10	−2.6	1811	321	714 ± 5%	863 ± 5	−149 ± 7
P55Mg24Ca16Na5	−2.3	1910	305	751 ± 5%	974 ± 5	−223 ± 11
P40Mg24Ca16Na15Fe5	−4.1	2366	319	704 ± 3%	925 ± 5	−221 ± 7
P45Mg24Ca16Na10Fe5	−3.5	2185	330	730 ± 3%	957 ± 5	−227 ± 8
P50Mg24Ca16Na5Fe5	−3.1	2257	329	775 ± 4%	877 ± 5	−102 ± 4
P55Mg24Ca16Fe5	−2.8	2462	329	839 ± 4%	1000 ± 5	−161 ± 7

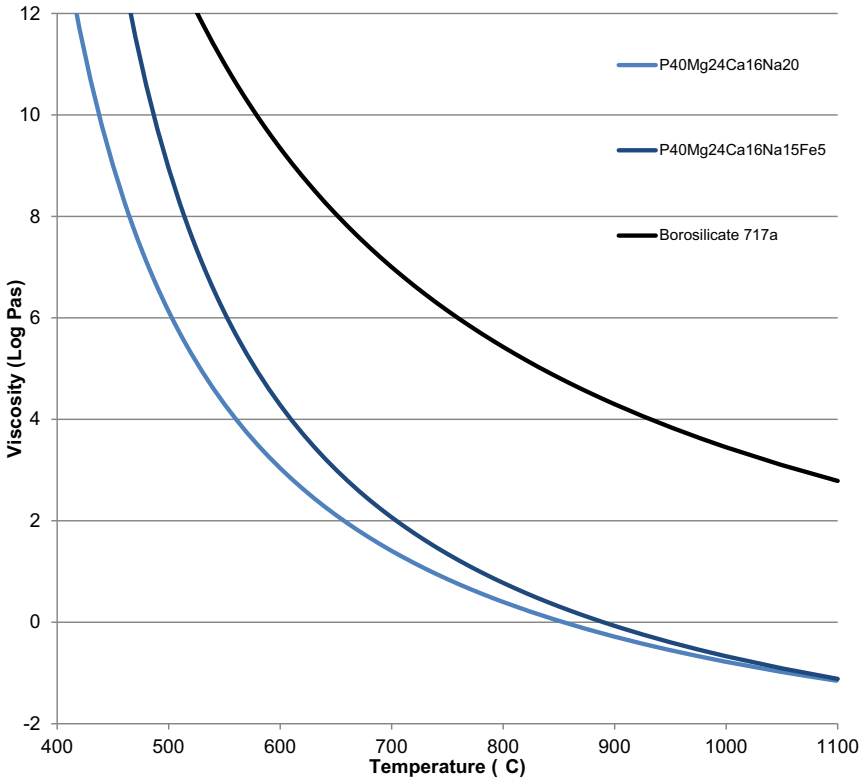

Fig. 6. Combined viscosity profiles fitted using the Vogel–Fulcher–Tammann equation for the P40Mg24Ca16Na20 and P40Mg24Ca16Na15Fe5 glasses, with the standard glass 717a for comparison. Errors are taken to be ±0.2 Log Pa·s.

5% Fe_2O_3 or, at least, the magnitude of the effect of the presence of the iron masks the effect of the phosphorous.

By plotting the values of drawing point temperature (T_D) against phosphate content of the glass, there is a very good correlation (Fig. 7). The non-iron containing glass and the iron containing glass each appear to follow closely to a polynomial fit, with the iron pushing up the drawing point by a considerable amount. However the fit has no particular basis and is certainly dependent on the modifier component of the glass and so its predictive capacity is limited.

The borosilicate glass is provided for reference. It typically has a higher viscosity than the phosphate glass by several decades, highlighting what was said in Section 4.2.1.

4.3. Fragility

The data can also be used to obtain fragility indices, or relative values of the fragility of the glasses. Fragility gives an indication of the rate of change of the viscosity of the glass with temperature, which is an

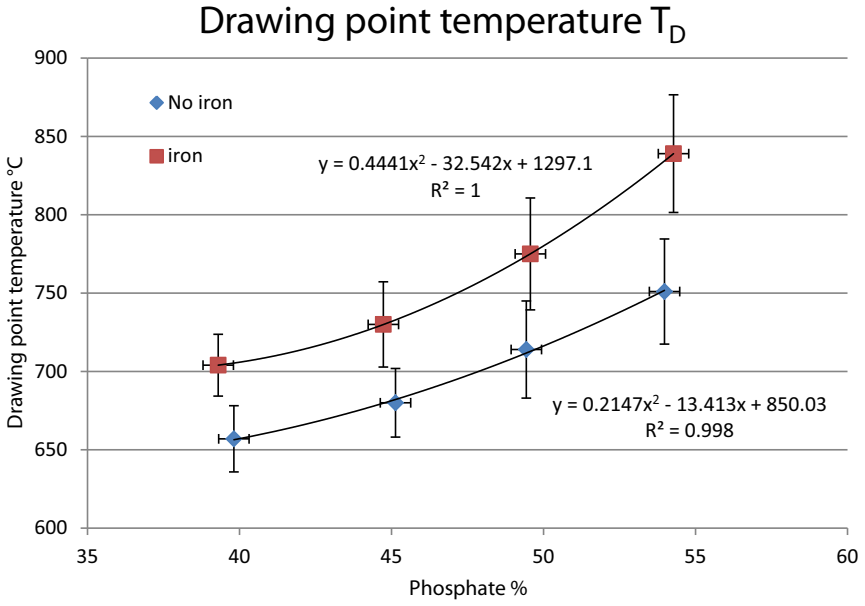

Fig. 7. Drawing point temperatures (T_D) as a function of phosphate content for the iron containing and non-iron containing glasses.

Table 5
Activation energies and Doremus Fragility Index.

Glass code (mol% oxide)	Q_H (kJ/mol)	Q_L (kJ/mol)	R_D
P40Mg24Ca16Na20	570 ± 1	157 ± 1	3.64 ± 0.02
P45Mg24Ca16Na15	577 ± 1	144 ± 1	3.99 ± 0.03
P50Mg24Ca16Na10	583 ± 1	149 ± 1	3.90 ± 0.03
P55Mg24Ca16Na5	513 ± 1	150 ± 1	3.42 ± 0.02
P40Mg24Ca16Na15Fe5	639 ± 1	193 ± 1	3.30 ± 0.02
P45Mg24Ca16Na10Fe5	616 ± 1	164 ± 1	3.75 ± 0.02
P50Mg24Ca16Na5Fe5	572 ± 1	179 ± 1	3.19 ± 0.02
P55Mg24Ca16Fe5	548 ± 1	186 ± 1	2.94 ± 0.02
Borosilicate 717a	453 ± 1	231 ± 1	1.96 ± 0.01

Table 6
Angell Fragility Parameters.

Glass code (mol% oxide)	T_g from VFT	Angel (m — extrapolated)	Angel (m — calculated)	$F_{1/2}$
P40Mg24Ca16Na20	417 ± 2	59 ± 1	47 ± 2	0.440 ± 0.006
P45Mg24Ca16Na15	429 ± 2	63 ± 1	51 ± 3	0.445 ± 0.006
P50Mg24Ca16Na10	445 ± 2	62 ± 1	52 ± 3	0.441 ± 0.007
P55Mg24Ca16Na5	439 ± 2	53 ± 1	47 ± 3	0.381 ± 0.007
P40Mg24Ca16Na15Fe5	466 ± 2	62 ± 1	51 ± 2	0.482 ± 0.006
P45Mg24Ca16Na10Fe5	471 ± 2	59 ± 1	51 ± 3	0.463 ± 0.007
P50Mg24Ca16Na5Fe5	479 ± 2	56 ± 1	48 ± 2	0.423 ± 0.007
P55Mg24Ca16Fe5	495 ± 3	51 ± 1	44 ± 2	0.380 ± 0.007
Borosilicate 717a	526 ± 5	29 ± 1	23 ± 1	0.259 ± 0.007

important parameter in glass drawing — a high fragility requires a much tighter control of processing conditions so that the operation can be held in a much smaller operating window. Fragility can be measured in a number of ways and in this study we will consider three approaches, one by Doremus and two by Angell.

4.3.1. Doremus

At both high and low temperatures, the value of T_0 in the VFT equation (Eq. (1)) approaches 0 and simplified Equations of activation energy can be applied to obtain the high temperature (Q_H) and low temperature (Q_L) activation energies via Eq. (2).

$$\eta = A \cdot \exp\left(\frac{Q}{RT}\right) \tag{2}$$

The ratio of these activation energies provides what is referred to as the Doremus fragility ratio (R_D), with higher values indicating a more fragile glass [14]. If a VFT fit is applied individually to the real data sets (quasi static and bob-in-up) the absolute value of T_0 is <1 in each case, and so the data has been considered sufficiently linear for the activation energy fit to be used. The activation energies and resulting R_D values are provided in Table 5. The Q_L values fall within a range similar to that observed via fibre elongation tests by Abe [25].

It is quite clear that the phosphate glasses are more fragile than the borosilicate, but this is as expected. It is interesting to note that rather than a gradual decrease in fragility as the phosphate content goes from 40 to 55%, there actually appears to be a peak in fragility at 45% before it drops away again. This is the case for both the iron containing and non-iron containing glasses. The introduction of iron appears to reduce the fragility of the glass in all cases.

4.3.2. Angell

An alternative measurement of fragility is offered by Angell, who used a reduced plot of T_g/T to compare glasses directly in terms of their viscosity gradient near T_g. This causes difficulty in that by its very nature T_g is a rate dependent value and so does not have an equilibrium value. However for practical purposes it is typically the case that a heating rate of 10 °C/min is used to determine T_g. Graphs of Log(η) against T_g/T are provided in Fig. 8.

What is immediately apparent from Fig. 8 is that the values of viscosity at T_g in this reduced plot are in the region of 9–10 Log Pa·s. A general rule for non-fragile glasses is that viscosity is expected to be on the order of 12 Log Pa·s at the T_g [26]. While Moynihan has shown that this does not hold for fragile glasses [27], a value of 9–10 seems very low, particularly in view of the recent results of Muñoz-Senovilla, who observed viscosities of greater than 12 Log Pa·s for metaphosphates at T_g when measured directly via beam bending [28]. The results of Muñoz-Senovilla do fit with the suggestions from Ropp that phosphate glasses need to be annealed 10 °C above T_g [16]. Ultimately this suggests that the 10 °C/min heating rate to obtain the T_g for this plot is not appropriate. Černošek demonstrated that the difference between T_g taken at 10 °C/min and 'equilibrium' T_g can be considerable in chalcogenide glasses [26] and it is not unreasonable to consider that this could be true for phosphate glasses as well.

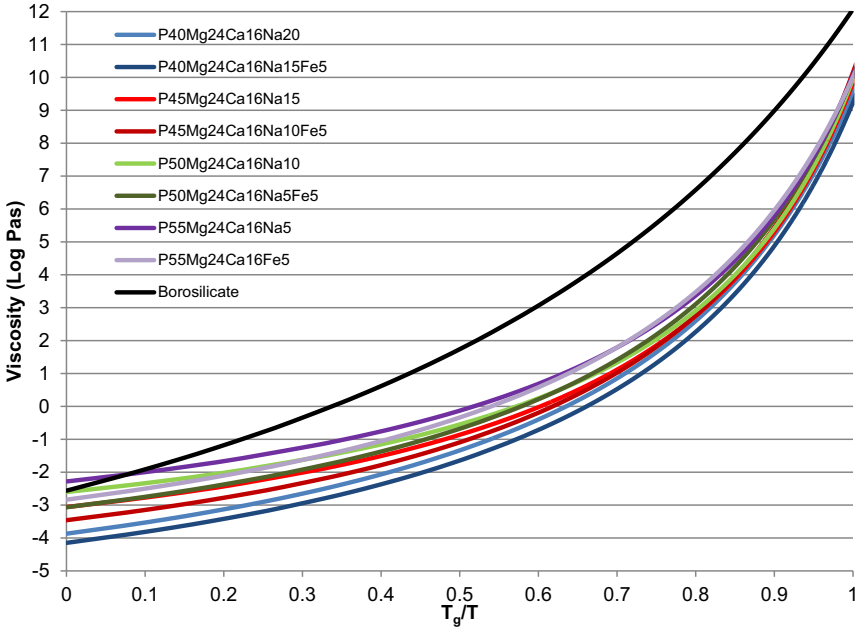

Fig. 8. Viscosity plotted against reduced temperature (T_g/T), with the standard glass for comparison. Errors are taken to be ±0.2 Log Pa·s.

In order to address this, the VFT parameters in Table 4 were used to determine values of T at a viscosity of 12 Log Pa·s and this was then taken to be the 'equilibrium' T_g. While this is not strictly speaking correct, it provides a useful method of normalisation for comparison of fragility with the standard glass. These 'equilibrium' T_g values are provided in Table 6 and were used to re-normalise the η vs T_g/T plot, which is shown in Fig. 9.

The first approach used by Angell to consider fragility is the most well-known assessment of fragility, 'm', which is the gradient of the reduced temperature plot at T_g (Eq. (3) [12]).

$$m = \left[\frac{\partial \mathrm{Log}_{10}\eta}{\partial\left(\frac{T_g}{T}\right)}\right]_{T=T_g} \tag{3}$$

This can be obtained quite simply from the extrapolated plot, though as Angell notes this measurement can be subjective, particularly in glasses with a rapid change in viscosity at this point, and so the value of 'm' can also be calculated from the VFT parameters by using Eq. (4) [13]. Both these values are provided in Table 6.

$$m = B \cdot T_g \cdot \left(T_g - T_0\right)^{-2} \tag{4}$$

The second approach used by Angell (and Richert) to consider fragility is by using a measure of deviation from Arrhenius behaviour and is referred to as $F_{1/2}$, shown in Eq. (5) [13], where $T_{1/2}$ is the value of T at a viscosity of 3.5 Log Pa·s. In essence it measures the distance of the curve away from the ideal state at a halfway point between 12 Log Pa·s and −5 Log Pa·s (generally considered a lower common limit of viscosity), with a value of 0 being an ideally strong glass and a value of 1 being an ideally weak glass. The values of $F_{1/2}$ are provided in Table 6.

$$F_{\frac{1}{2}} = \frac{2T_g}{T_{\frac{1}{2}}} - 1 \tag{5}$$

Comparison of the fragility parameter from Doremus with those of Angell and Richert shows a largely similar trend. The values are plotted in Fig. 10a and b for clarity. All the glasses are significantly more fragile than the Borosilicate 717a standard glass.

The result in Fig. 10a is somewhat unexpected. An increase in phosphate chain length would be expected to reduce the fragility, since it would take more time for the longer chains to rearrange and relax, and more so with greater branching. This would appear to be the case moving from P45 to P50 to P55 but there is an apparent drop in the fragility at P40. However, it is difficult to assign an uncertainty to these fragility parameters and so the lower value may not be statistically significant. In fact, this lower value may be representative of the level of uncertainty as there is no factor that could (in the author's opinion) cause the fragility of P40 to be lower. Even considering this, the P55 value does appear to be significantly lower than the rest. Since the P50 actually has slightly lower than 50% phosphate content, the P55 is the only glass expected to have very long phosphate chains [29].

The result in Fig. 10b seems to be more clear, with a general reduction in fragility except for the Doremus value for the P45 glass. As was seen in in Fig. 5, iron has a strong effect on the viscosity at lower temperatures, in the range where m is measured. However, the absolute change in the fragility is quite small with the addition of iron, which is surprising. As postulated previously, this may be related to the mobility of iron in the glass and bears further investigation.

5. Conclusions

The quasi static and bob-in-cup viscosity data fit well to the Vogel Fulcher Tammann equation, providing an estimation of drawing point temperatures of between 657 and 839 °C. The drawing point temperature follows an increasing trend with phosphate content and the presence of iron also increases the drawing point. No glasses achieved a positive ΔT value. Overall, the viscosity of the glasses increases with phosphate content, but the effect may be limited at low temperature. The presence of iron increases the viscosity at low temperature but has only a small effect at high temperature. All the glasses were of considerably lower viscosity than the borosilicate 717a standard glass.

It is difficult to determine an appropriate T_g value suitable for a reduced temperature plot, a DSC heating rate of 10 °C/min appears to be too fast for these glasses. Use of an 'equilibrium' T_g value from the VFT fit enables a more useful comparator. All the glasses were of considerably higher fragility than the borosilicate 717a standard glass. The fragility of the iron free glasses appeared to increase significantly only when the phosphate content is >50%. Iron has a limited effect on fragility.

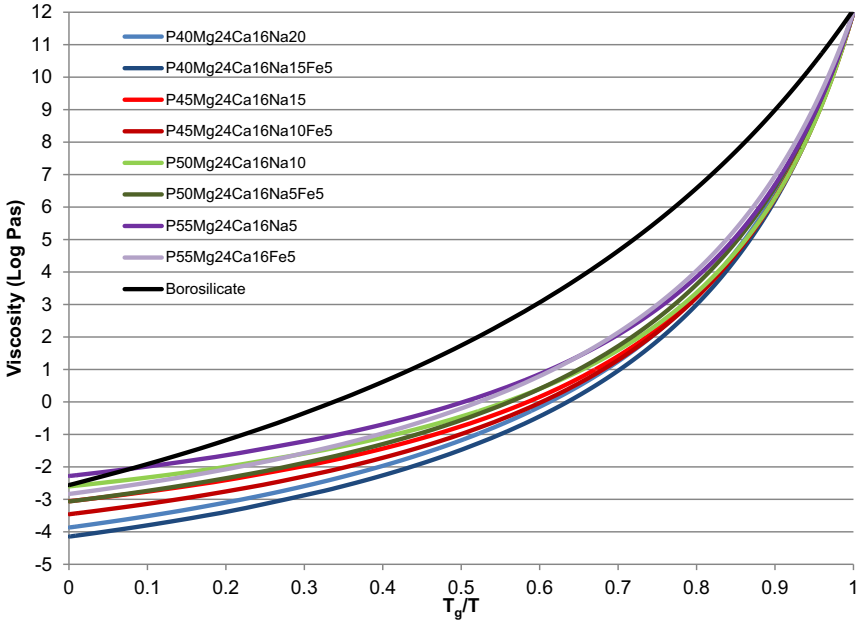

Fig. 9. Viscosity plotted against reduced temperature (T_g/T) using the 'equilibrium' T_g values obtained from the VFT parameters. Errors are taken to be ±0.2 Log Pa·s.

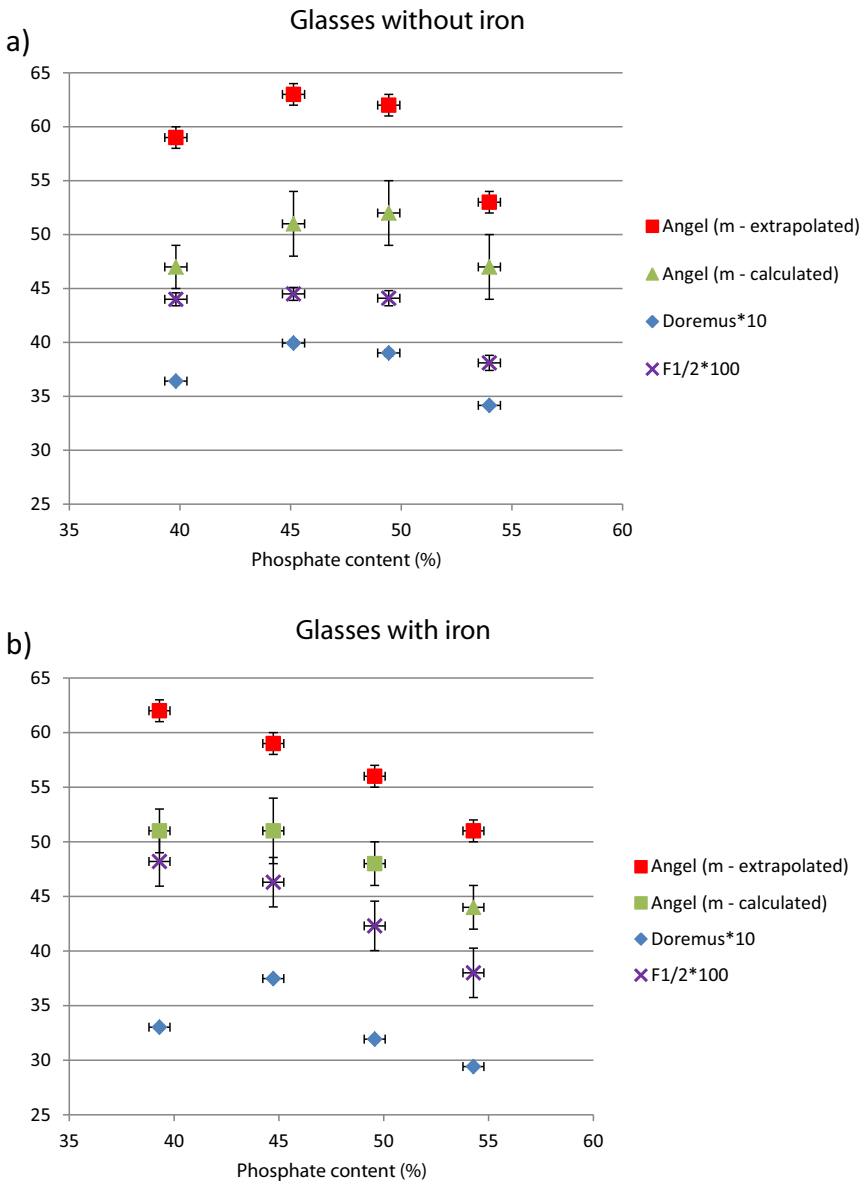

Fig. 10. a. Fragility parameters for the glasses that do not contain iron, as a function of phosphate content. Multiplication factors have been used to allow for easier comparison. b. Fragility parameters for the glasses that contain iron, as a function of phosphate content. Multiplication factors have been used to allow for easier comparison.

Borosilicate 717a is a poor standard material in the conditions that were used, due to a continuous change in viscosity over time.

Acknowledgements

The authors would like to thank the Technology Strategy Board (project #101227) for providing funding to support this study, and to Dr David Furniss of the University of Nottingham for his advice.

References

[1] A.J. Parsons, I. Ahmed, P. Haque, B. Fitzpatrick, M.I.K. Niazi, G.S. Walker, C.D. Rudd, J. Bionic Eng. 6 (2009) 318–323, http://dx.doi.org/10.1016/S1672-6529(08)60132-8.
[2] J.C. Knowles, J. Mater. Chem. 13 (2003) 2395–2401, http://dx.doi.org/10.1039/b307119g.
[3] D.S. Brauer, C. Rüssel, S. Vogt, J. Weisser, M. Schnabelrauch, J. Mater. Sci. Mater. Med. 19 (2008) 121–127, http://dx.doi.org/10.1007/s10856-007-3147-x.
[4] N. Sharmin, A.J. Parsons, C.D. Rudd, I. Ahmed, J. Biomater. Appl. (June 17 2014), http://dx.doi.org/10.1177/0885328214539824 (published online).
[5] B.C. Bunker, J. Non-Cryst. Solids 64 (1983) 291–316, http://dx.doi.org/10.1016/0022-3093(84)90184-4.
[6] P. Haque, I. Ahmed, A.J. Parsons, R. Felfel, G.S. Walker, C.D. Rudd, J. Non-Cryst. Solids 375 (2013) 99–109, http://dx.doi.org/10.1016/j.jnoncrysol.2013.05.008.
[7] D. Hewak (Ed.), Properties, Processing and Applications of Glass and Rare Earth-doped Glasses for Optical Fibres, IEE: INSPEC, London, 1998 (ebook).
[8] F.T. Wallenberger, J.C. Watson, H. Li, in: D.B. Miracle, S.L. Donaldson (Eds.), ASM Handbook, Vol. 21: CompositesASM International, Ohio, 2001, pp. 27–34.
[9] J.M. Stickel, M. Nagarajan, Int. J. Appl. Glass Sci. 3 (2012) 122–136, http://dx.doi.org/10.1111/j.2041-1294.2012.00090.x.
[10] F.T. Wallenberger, in: F.T. Wallenberger, P.A. Bingham (Eds.), Fiberglass and Glass Technology, Springer, US, 2010, pp. 3–90, http://dx.doi.org/10.1007/978-1-4419-0736-3.
[11] A.N. Gent, Br. J. Appl. Phys. 11 (1960) 85–87, http://dx.doi.org/10.1088/0508-3443/11/2/310.
[12] R. Böhmer, C.A. Angell, Phys. Rev. B 45 (1992) 10091–10994, http://dx.doi.org/10.1103/PhysRevB.45.10091.
[13] R. Richert, C.A. Angell, J. Chem. Phys. 108 (1998) 9016–9026, http://dx.doi.org/10.1063/1.476348.
[14] R.H. Doremus, Am. Ceram. Soc. Bull. 82 (2003) 59–63.
[15] M.S. Hasan, I. Ahmed, A.J. Parsons, G.S. Walker, C.A. Scotchford, J. Mater. Sci. Mater. Med. 23 (2012) 2531–2541, http://dx.doi.org/10.1007/s10856-012-4708-1.
[16] R.C. Ropp, Studies in Inorganic Chemistry 15: Inorganic Polymeric Glasses, Elsevier Science Publishers B.V., Amsterdam, 1992.
[17] S.J. Wilson, D. Poole, Mater. Res. Bull. 25 (1990) 113–118, http://dx.doi.org/10.1016/0025-5408(90)90170-7.
[18] A.B. Seddon, V.K. Tikhomirov, H. Rowe, D. Furniss, J. Mater. Sci. Mater. Electron. 18 (2007) S145–S151, http://dx.doi.org/10.1007/s10854-007-9190-z.

[19] S.I.S. Shaharuddin, I. Ahmed, D. Furniss, A.J. Parsons, C.D. Rudd, Glass Technol. Part A 53 (2012) 245–251.
[20] R.K. Brow, C.M. Arens, X. Yu, E. Day, Phys. Chem. Glasses 35 (1994) 132–136.
[21] A.J. Parsons, C.D. Rudd, J. Non-Cryst. Solids 354 (2008) 4661–4667, http://dx.doi.org/10.1016/j.jnoncrysol.2008.05.050.
[22] A. Napolitano, E.G. Hawkins, J. Res. Natl. Bur. Stand. A Phys. Chem. 68A (1964) 439–447, http://dx.doi.org/10.6028/jresv68An5p439_A1b.
[23] A. Napolitano, E.G. Hawkins, Viscosity of a standard borosilicate glass, National bureau of standards special publication 260-231970.
[24] M.I. Ojovan, Adv. Condens. Matter Phys. 2008 (2008), http://dx.doi.org/10.1155/2008/817829 (Article ID 817829, 23 pages).
[25] Y. Abe, in: M. Grayson, E.J. Griffith (Eds.), Topics in Phosphorus Chemistry, vol. 11, John Wiley & Sons, New York, 1983, pp. 19–67.
[26] Z. Černošek, J. Holubová, E. Černošková, M. Liška, J. Optoelectron. Adv. Mater. 4 (2002) 489–503.
[27] C.T. Moynihan, J. Am. Ceram. Soc. 76 (1993) 1081–1087, http://dx.doi.org/10.1111/j.1151-2916.1993.tb03724.x.
[28] L. Muñoz-Senovilla, F. Muñoz, J. Non-Cryst. Solids 385 (2014) 9–16, http://dx.doi.org/10.1016/j.jnoncrysol.2013.10.021.
[29] E.J. Griffith, Phosphate Fibers, Plenum Press, New York, 1995.